Journal of Alloys and Compounds 527 (2012) 132–136

Contents lists available at SciVerse ScienceDirect

Journal of Alloys and Compounds

journal homepage: www.elsevier.com/locate/jallcom

Titania nanotube synthesized by a facile, scalable and cheap hydrolysis method for reversible lithium-ion batteries

Bin Wang [a,*], Jianli Cheng [b], Yuping Wu [a]

[a] Department of Chemistry and Shanghai Key Laboratory of Molecular Catalysis and Innovative Materials, China
[b] Department of Macromolecular Science, Fudan University, No. 220, Handan Road, Shanghai 200433, China

ARTICLE INFO

Article history:
Received 4 December 2011
Received in revised form 16 February 2012
Accepted 17 February 2012
Available online xxx

Keywords:
Lithium ion batteries
Cycle ability
Titania
Nanotubes
Anode

ABSTRACT

Here, we report a facile, scalable, and cheap hydrolysis method for preparing titania nanotube material by using the cellulose filter paper as the template, which can be applicable to anode materials of Li-ion batteries. The electrochemical performances show that titania nanotube anodes have improved lithium-ion storage ability, enhanced charge–discharge kinetics, and prolonged cycling life compared with titania particles obtained from sol–gel method.

1. Introduction

Lithium-ion batteries (LIBs) have been widely used in many aspects of our society, such as mobile phone, laptop computer, and digital camera. However, the sustainable energy density and power density of LIBs are still much lower than the requirements of vehicle application, especially for electric vehicles (EV) and plug-in hybrid electric vehicles (PHEV) [1–7]. As for commercial LIBs, graphite is typically used as an anode material. However, there are inevitably safety problems for LIBs due to the possible production of lithium metal dendrites during continuous charge–discharge process. So much work has been done to investigate the electrochemical performance of potential anode for satisfying the requirements of high-performance batteries for EV and PHEV. Among the potential anode candidates, TiO_2 has been widely investigated because it can be versatile used in many different fields, such as semiconductors, photocatalysts, photovoltaic devices, gas sensing, and energy storage and conversion [8–12]. Especially, TiO_2 as an anode of LIB has attracted much attention due to its high lithium insertion potential to avoid the formation of lithium dendrite, high stability, environmental benign, low cost and the ability to be prepared with different morphology, such as spheres [12–14], nanofibers [15], nanoribbons [16], and nanotubes [17–19].

Compared with the conventional materials, nanostructure materials have some substantial advantage. Both electron and Li-ion transport path are much shorter, which can facilitate the electrochemical process. At the same time, they can accommodate the volume expansion during the intercalation/deintercalation process. Furthermore, higher electrode–electrolyte contact area helps to get better electrochemical performance. Among the one-dimensional nanostructures, nanotubes are better than nanofibers and nanorods as electrode materials because both their inner and outer surfaces can contact with the electrolyte, which is beneficial to the electrochemical performance. Furthermore, the void spaces inside the nanotubes also eliminate the stress of volume change during the intercalation/deintercalation process and hence provide good performance. Wang et al. [19] prepared mesoporous titania nanotube by using the anodic aluminum oxide (AAO) and P123 as the hard and soft template, respectively. The electrochemical testing results show that mesoporous titania nanotubes have a good performance. Recently, Kyerematen et al. [20] investigated the performance of titania nanotube electrodes with electropolymerized copolymer electrolyte for 3D microbatteries. Bae et al. [21] demonstrated the improved performance of amorphous titania nanotubes with self-branched crystalline nanorods prepared by atomic layer deposition combined with the template-directed approach. Furthermore, several studies have shown that carbon coated [22] or nitridated [23] TiO_2 nanotubes can improve reversible capacity by suppression the nanotube agglomeration. More recently, Pandaa et al. [24] reported the performances of TiO_2 nanotubes with different wall thickness by atomic layer deposition

* Corresponding author at: Lawrence Berkeley National Lab, USA.
Tel.: +1 510 486 7084; fax: +1 510 486 7084.
E-mail address: binwang@lbl.gov (B. Wang).

0925-8388/$ – see front matter © 2012 Elsevier B.V. All rights reserved.
doi:10.1016/j.jallcom.2012.02.108

using AAO membranes as the template. However, most of them take advantage of the expensive hard-template such as AAO or the molecular soft template such as polymer/copolymer surfactant combined with complex process. The simple, inexpensive and scalable fabrications of TiO_2 nanotubes are still a challenge because of the cost of template, limited product yield, and the complexity of the methods. Herein, we report a simple and inexpensive method to prepare the titania nanotubes by using ordinary ashless cellulose filter paper as the template and their application in a rechargeable lithium ion battery. When titania nanotube used as anode of LIB, it shows excellent electrochemical charge/discharge behavior.

2. Experimental

2.1. Preparation of nanotube

0.255 g of $Ti(OBu)_4$ were dissolved in 25 mL of an anhydrous ethanol solvent with small amount of acetic acid. A piece of filter paper was placed in this solution for a while to ensure certain adsorption amount of titanate on the surface of filter paper, and was washed by ethanol, followed by drying with nitrogen flow. Then the filter paper was transferred into a beaker with copious de-ionized water, covered and kept for several hours to let the titanate hydrolysis thoroughly at room temperature. The as-prepared titania/filter paper composite was subjected to calcinate in air at 500 °C for 3 h to remove the original filter paper. For comparison, the titania obtained from the sol–gel hydrolysis of $Ti(OBu)_4$ dissolving in an anhydrous ethanol solvent with small amount of acetic acid (pH value of 2–3) without using the cellulose filter paper also collected and calcinated. In both cases, white TiO_2 nanotubes or particles were obtained.

2.2. Nanotube characterization

The structures of the prepared titania were analyzed by X-ray diffraction (XRD, Panalytical Xpert Pro diffractometer with monochromatized Cu Kα radiation) and field emission scanning electron microscope (FESEM, JEOL7500). The cellulose paper and cellulose paper with the precursor were also characterized by thermogravimetric analysis (TGA Perkin ELEMER TGA7) and Fourier transform infrared spectroscopy (NICOLET 6700 FT-IR spectrometer). Surface area analysis was carried out by using the BET nitrogen adsorption method (Micromeritics Instrument Corporation TriStar II 3020).

2.3. Electrochemical testing

The electrode was prepared as follows: active material, carbon black and polyvinylidene difluoride (PVDF) was mixed in N-methyl-2-pyrrolidone as solvent to prepare slurry with the weight ratio of 7:2:1. The slurry was coated on an aluminum foil, and then heated in a vacuum oven at 100 °C for overnight. The density of electrode used in this experiment was 3–5 mg cm^{-2}. The electrolyte was 1 M $LiPF_6$ dissolved in a 1:1 (v/v) mixture of ethylene carbonate (EC) and diethyl carbonate (DEC). Electrochemical performance of the electrode was determined with 2032 coin-type cells with lithium foil as the counter and reference electrode, and Celgard 2500 as the separator. The cell was assembled in a glove box under a dry argon atmosphere and tested by an Arbin battery testing system 2.0 in the voltage range of 1–3 V vs. Li^+/Li at different current density. The C-rate was based on a reversible lithium-ion deintercalation capacity of 185 mAh g^{-1}. The lithium-ion deintercalation from the electrode defined as the charge process. Cyclic voltammograms were carried out at different scan rates with Solartron Instrument model 1287 controled by a computer.

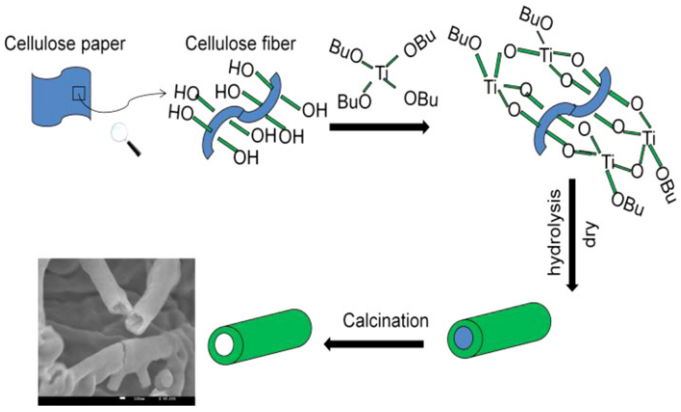

Fig. 1. Schematic illustration of the synthetic procedure used for the titania nanotube.

3. Results and discussion

Compared to the reported preparation processes [18,19,26], the titania nanotubes in this study were produced directly by the hydrolysis of titanate without adding any additional capping agent to form a homogeneous precursor. The schematic illustration of the synthetic procedure used for preparing the titania nanotube by a simple hydrolysis route is shown in Fig. 1. The reaction processes involving the hydrolysis and condensation between TiO_2 precursor and the hydroxyl groups from the surface of filter fiber are as follows:

$$Ti(OBu)_4 + 2HOCH_2CH_3 \rightarrow Ti(OCH_2CH_3)_2 + 4BuOH$$

$$Ti(OCH_2CH_3)_2 + 2H_2O \rightarrow Ti(OH)_2 + 2HOCH_2CH_3$$

$$Ti(OH)_2 + 2HO{-}Fiber \rightarrow 2Fiber{-}O{-}Ti{-}O{-}H + 2H_2O.$$

Nanotubular TiO_2 was obtained after removal of the organic substances by calcination. The interaction between the titanate precursor and the cellulose filter paper was confirmed by IR spectroscopy. FTIR spectra of cellulose paper, cellulose paper with the precursor, and the prepared titania are shown in Fig. 2 (a). Strong O—H stretching vibration (3430 cm^{-1}), CH_2 stretching vibration

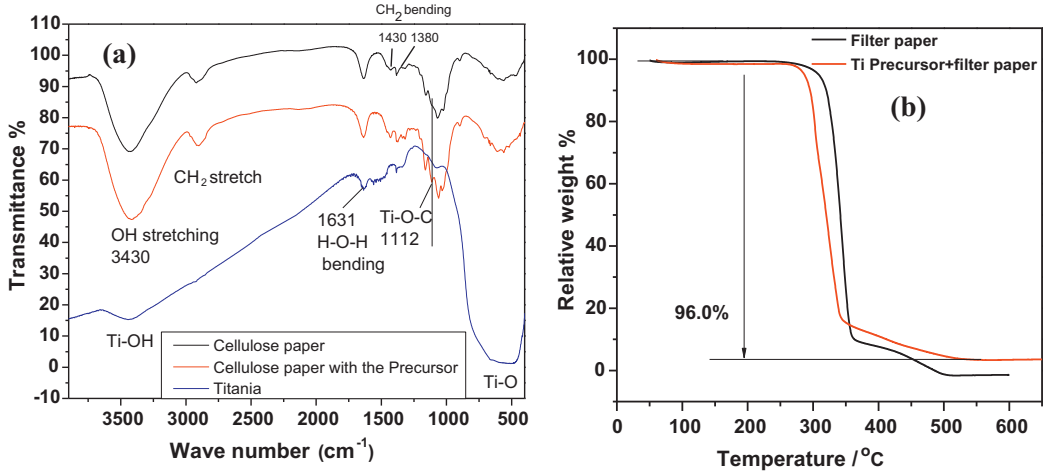

Fig. 2. (a) FTIR spectra of cellulose paper, cellulose paper with the precursor, and the prepared titania; (b) TGA plots of pure filter paper and filter paper with the precursor.

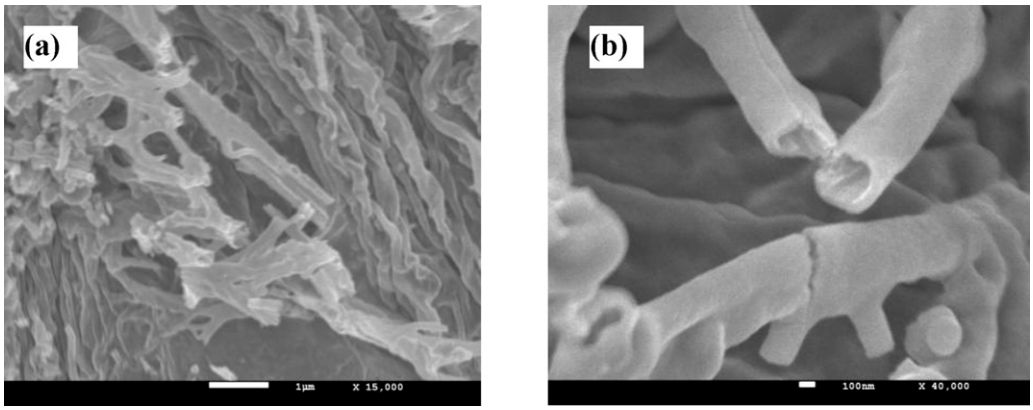

Fig. 3. SEM images of titania nanotube at different magnification after annealing at 500 °C in air.

(2910 cm^{-1}) and bending vibration (1430 cm^{-1} and 1380 cm^{-1}) peaks are observed for both cellulose paper and cellulose paper with the precursor. The IR spectra of cellulose paper with the precursor exhibits a new peak at 1112 cm^{-1} due to Ti—O—C stretching vibration [26,27]. This peak does not present before the interaction with the precursor and after the annealing of the cellulose paper. In the spectra of the titania after annealing, the small peak at 3413 cm^{-1} is due to the stretching vibration of Ti—O—H, and the bending vibration of H—O—H from the absorbed water on the surface could be found at 1626 cm^{-1}. A broad peak at 500–750 cm^{-1} is attributed to Ti—O—Ti stretching vibration, which is consistent with the reported results of titania [25,26,28]. Thermogravimetric analysis (TGA) plots recorded in air with a heating rate of 10 °C min^{-1} are compared in Fig. 2(b). No weight remain is observed in the cases of pure cellulose filter paper. The weight loss of filter paper with the precursor is 96%, which can be attributed to the removal of filter paper and the crystalline of adsorbed titania. It is worth noting that the adsorbed amount of titanate on the filter paper can be controled by the repeat times of depositing and coating cycle.

The morphology of cellulose filter paper can be seen in Fig. S1 in ESI. It is clear that there are many cellulose fibers in the template. Without using the cellulose filter paper, only the agglomerations of TiO_2 particles were obtained (shown in Fig. S2 in ESI). Fig. 3 shows the scanning electron microscopy (SEM) images of the titania nanotube obtained by the synthesis process described at different magnification after annealing at 500 °C in air. It can be known from these images that nanotubes whose visible open ends were shown in the imaging region confirmed the nanotubular structure. TEM images of TiO_2 nanotube at different magnification also confirmed the tubular structure (shown in Fig. S3 in ESI). It is interesting to note that the TiO_2 nanotubes stay in close contact each other to partially form the nanotubular titania array unlike the reported titania tube dispensing randomly with the assistance of surfactant.

Fig. 4(a) shows the X-ray diffraction (XRD) patterns of the obtained titania nanotube. All of the peaks correspond to anatase titania phase (JCPDS 84-1285) that have reduced intensity of the diffraction peaks. No other crystalline phases were detected, which demonstrates that the precursor was totally removed by the calcination process. Calculated by using Scherrer's formula, the average crystallite size of titania in the titania nanotube is approximately 4 nm. The nitrogen adsorption–desorption isotherm shows that the titania nanotube sample has a Brunauer–Emmett–Teller (BET) surface area of 24.5 $m^2\ g^{-1}$. It is higher than the estimated value of 21.4 $m^2\ g^{-1}$ for 200 nm hexagonal closest packed pore and close to that of reported ordered mesoporous titania synthesized by polystyrene colloidal crystal as the template [26,29].

Fig. 4(b) shows the curves of cyclic voltammogram (CV) for the first four cycles. The profiles show one pronounced reduction/oxidation pair at 1.72/2.01 V, which is well consistent with the literature [26]. They should ascribe to the reversible intercalation/deintercalation of Li ion into/from the anatase. In the successive cycles, the plots of the CV keep almost same (the ratio of anodic and cathodic peak current is nearly 1 with the peak separation of 0.29 V), which demonstrates that the process of lithium-ion intercalation/deintercalation is very reversibly and reproduceable in the TiO_2 nanotube electrode. Fig. 5 (a) shows

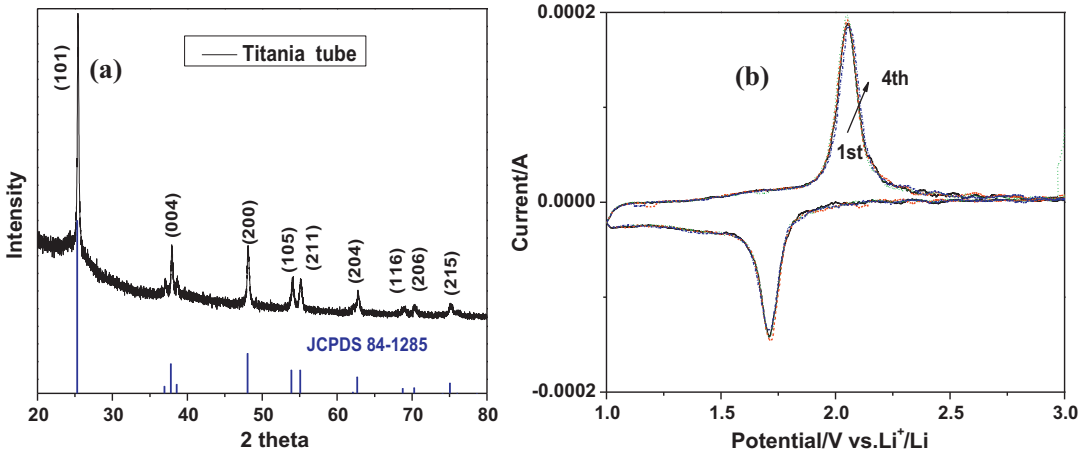

Fig. 4. (a) XRD patterns of the TiO_2 nanotube after annealing in air; (b) Cyclic voltammograms of the titania nanotube at a scan rate of 0.1 mV/s between 1.0 and 3.0 V.

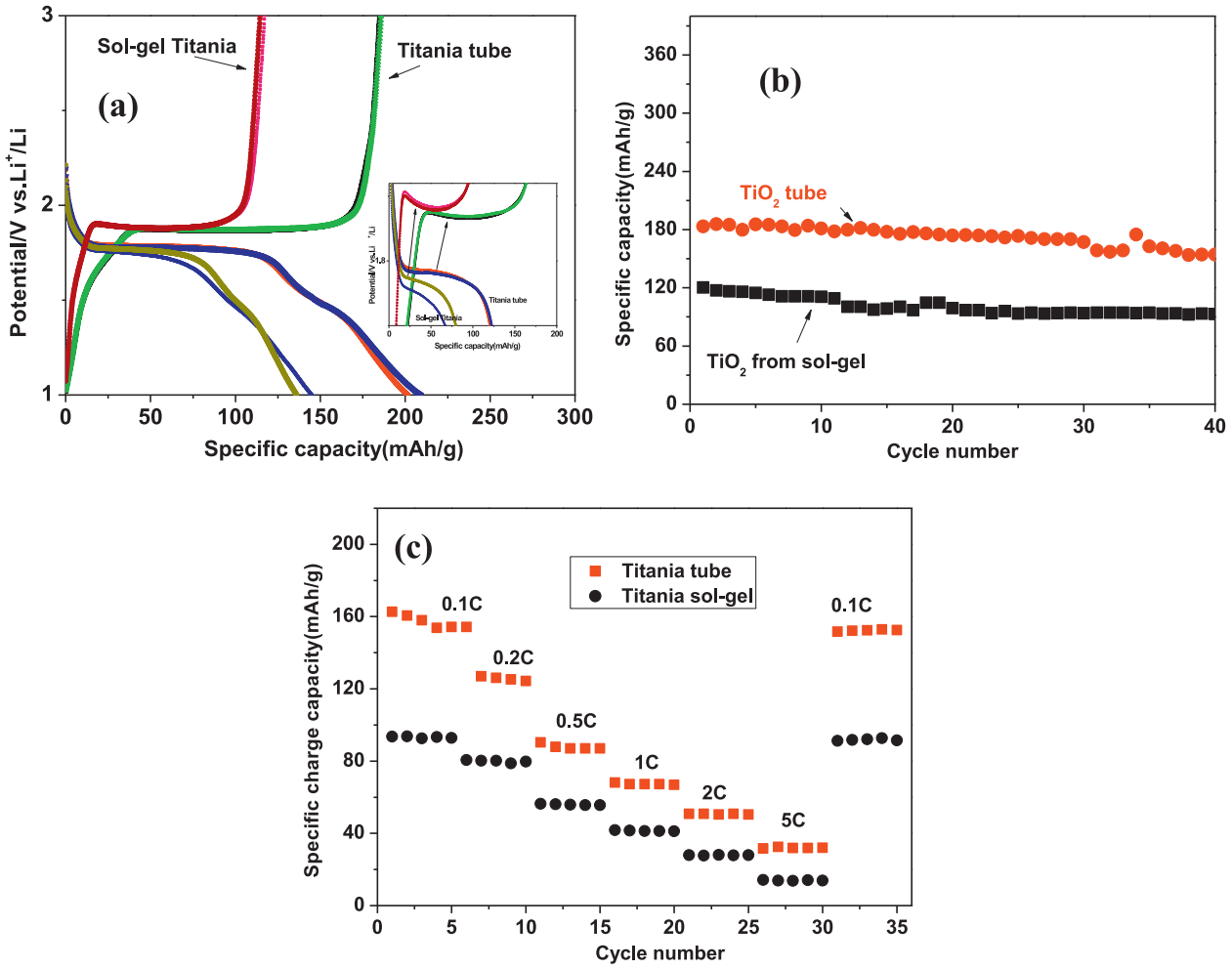

Fig. 5. (a) Charge–discharge profiles of the titania nanotube and titania obtained from sol–gel method at 0.1 C rate, the inset is the magnified profile; (b) Cycling performances of the TiO_2 nanotubes and TiO_2 obtained from sol–gel method at 0.1 C; and (c) Rate capability of the nanotube TiO_2 electrode and TiO_2 obtained from sol–gel at different rates ranging from 0.1 C to 5 C.

the charge–discharge profiles of the TiO_2 nanotube and titania obtained from sol–gel for the second and fifth cycles. It can be seen from the curves of titania nanotube that an obviously charge/discharge plateau regions at about 1.75 V can be identified in the charge/discharge process with a discharge capacity of 208 mAh g^{-1}, which is in agreement with the above CV results. As for the titania obtained from the sol–gel process, it can be seen that they show lower reversible capacity (136 mAh g^{-1}) and higher electrochemical polarization (larger separation between the oxidation and reduction plateau shown in inset). Interestingly, a new reversible process was found in the discharge profile of titania nanotube in 1.2–1.7 V regions (1.5–1.9 V regions in the charge process correspondingly), which may be attributed to the surface or interfacial lithium-ion storage of the nanomaterial [30,31]. The same phenomena also can be found in the differential capacity vs. voltage plot of the second and fifth cycles of the TiO_2 nanotube (shown in Fig. S4 in ESI). The reported results [32,33] have shown that this region is very sensitive to the TiO_2 particle size. Even though TiO_2 sample with the particle size of 140 nm, they still do not show the presence of second reversible region. These results are well consistent with the result of Scherrer's formula in the XRD. Cycling performances of synthesized TiO_2 nanotubes and TiO_2 obtained from sol–gel at 0.1 C are displayed in Fig. 5(b). It can be found that the TiO_2 nanotubes exhibit a higher charge capacity of 155 mAh g^{-1} after 40 cycles (only 92.8 mAh g^{-1} for titania obtained from sol–gel) with the excellent retention of 85% compared with the first reversible capacity. At the same time, the titania nanotubes also show better rate capability and reversibility at different rates ranging from 0.1 C to 5 C in Fig. 5 (c). The performance of TiO_2 nanotube is superior to that of the reported literatures [26,32–36], but further improving the rate capability can be obtained with coating carbon or conductive materials [22,23,33,34]. The improved electrochemical performances can be attributed to the following: the shorter lithium diffusion length of nanostructure, large electrode/electrolyte contact area, present a new reversible electrochemical insertion process due to the small particle size and better accommodation for strain change during the charge/discharge process.

It should be noted that compared with the results of metal oxide [1,3,5], the electrochemical capacity of titania anodes is somewhat lower because the titania has a theoretical maximum storage capacity of one lithium-ion. However, with the different transition metal precursor, the method could be easily applied to other metal oxide or common inorganic electrode material. We succeeded to prepare tin oxide nanotube by using the cellulose filter paper as the template. Further characterization is still under investigation. Meanwhile, the cellulose filter papers have been widely used in many aspects, so the cost of using the cellulose filter papers as the template to prepare the nanotubes is much lower than that of the known AAO template. Besides, the product yield of this method is much higher. Therefore, they are still promising for many potential applications in the future.

4. Conclusions

In summary, we report a facile method for large-scale synthesis of TiO_2 nanotubes by using cheap and commercial cellulose filter paper as the template. The obtained titania nanotubes used as anode material of LIB show excellent electrochemical charge/discharge behavior with a good rate capability. Although several researches of titania nanotubes by hard or soft template have been reported, the titania nanotubes synthesized by cellulose filter paper as the template have inherent advantage in view of basic properties of cellulose paper. The synthetic process is simple, cheap and scalable, which might be easily applicable to other metal oxide or common inorganic electrode material.

Acknowledgment

Financial support from National Basic Research Program of China (973 Program No: 2007CB209702) is greatly appreciated.

Appendix A. Supplementary data

Supplementary data associated with this article can be found, in the online version, at doi:10.1016/j.jallcom.2012.02.108.

References

[1] K.E. Aifantis, S.A. Hackney, R.V. Kumar, High Energy Density Lithium Batteries, Wiley, Weinheim, 2010.
[2] G.A. Nazri, G. Pistoia, Lithium Batteries Science and Technologies, Springer, New York, 2009.
[3] J.M. Tarascon, M. Armand, Nature 414 (2001) 359–367.
[4] S.A. Sherrill, P. Banerjee, G.W. Rubloff, S.B. Lee, Phys. Chem. Chem. Phys. 13 (2011) 20714–20723.
[5] C.M. Park, H.J. Sohn, Chem. Mater. 20 (2008) 6319–6324.
[6] Y.H. Yin, M.X. Gao, J.L. Ding, Y.F. Liu, L.K. Shen, H.G. Pan, J. Alloys Compd. 509 (2011) 10161–10166.
[7] X. Ji, K.T. Lee, L.F. Nazar, Nat. Mater. 8 (2009) 500–506.
[8] C. Encarnación Gómez, J.R. Vargas García, J.A. Toledo Antonio, M.A. Cortes Jacome, C. Ángeles Chávez, J. Alloys Compd. 495 (2010) 458–461.
[9] J. Tang, Y. Wu, E. McFarland, G. Stucky, Chem. Commun. 14 (2004) 1670–1671.
[10] J.H. Pan, X.S. Zhao, W.I. Lee, Chem. Eng. J. 170 (2011) 363–380.
[11] L.B. Fen, T.K. Han, N.M. Nee, B.C. Ang, M.R. Johan, Appl. Surf. Sci. 258 (2011) 431–435.
[12] H.S. Liu, Z.H. Bi, X.G. Sun, R.R. Unocic, M.P. Paranthaman, S. Dai, G.M. Brown, Adv. Mater. 23 (2011) 3450–3454.
[13] S. Yoon, A. Manthiram, J. Phys. Chem. C 115 (2011) 9410–9416.
[14] J.W. Hou, X.C. Yang, X.Y. Lv, M. Huang, Q.Y. Wang, J. Wang, J. Alloys Compd. 511 (2012) 202–208.
[15] A.R. Armstrong, G. Armstrong, J. Canales, R. Garcia, P.G. Bruce, Adv. Mater. 17 (2005) 862–866.
[16] T. Beuvier, M. Richard-Plouet, M. Mancini-Le Granvalet, T. Brousse, O. Crosnier, L. Brohan, Inorg. Chem. 49 (2010) 8457–8464.
[17] G. Armstrong, A.R. Armstrong, J. Canales, P.G. Bruce, Electrochem, Solid State Lett. 9 (2006) A139–A143.
[18] Y. Lan, X. Gao, H. Zhu, Z. Zheng, T. Yan, F. Wu, S. Ringer, D. Song, Adv. Funct. Mater. 15 (2005) 1310–1318.
[19] K. Wang, M. Wei, M.A. Morris, H. Zhou, J.D. Holme, Adv. Mater. 19 (2007) 3016–3020.
[20] N.A. Kyerematenga, F. Dumur, P. Knauth, B. Pecquenard, T. Djenizian, Electrochem. Commun. 13 (2011) 894–897.
[21] C. Bae, Y. Yoon, W.-S. Yoon, J. Moon, J. Kim, H. Shin, Appl. Mater. Interface 2 (2010) 1581–1587.
[22] S.J. Park, Y.J. Kim, H. Lee, J. Power Sources 196 (2011) 5133–5137.
[23] H. Han, T. Song, J.Y. Bae, L.F. Nazar, H.S. Kim, U. Paik, Energy Environ. Sci. 4 (2011) 4532–4536.
[24] S.K. Pandaa, Y. Yoona, H.S. Jungb, W.S. Yoon, H. Shina, J. Power Sources 204 (2012) 162–167.
[25] G. Sudant, E. Baudrin, D. Larcher, J.M. Tarascon, J. Mater. Chem. 15 (2005) 1263–1269.
[26] L.J. Fu, T. Zhang, Q. Cao, H.P. Zhang, Y.P. Wu, Electrochem. Commun. 9 (2007) 2140–2144.
[27] G.Q. Liu, Z.G. Jin, X.X. Liu, T. Wang, Z.F. Liu, J. Sol–Gel Sci. Technol. 41 (2007) 49–55.
[28] C. Lai, G.R. Li, Y.Y. Dou, X.P. Gao, Electrochim. Acta 55 (2010) 4567–4572.
[29] Z. Wang, J. Chen, T. Zhu, S. Madhavi, X. Lou, Chem. Commun. 46 (2010) 6906–6908.
[30] P. Kubiak, J. Geserick, N. Husing, M. Wohlfahrt-Mehrens, J. Power Sources 175 (2008) 510–516.
[31] Y. Ren, L. Hardwick, P.G. Bruce, Angew. Chem. Int. Ed. 49 (2010) 2570–2574.
[32] M.V. Reddya, R. Joseb, T.H. Tengb, B.V.R. Chowdari, S. Ramakrishna, Electrochim. Acta 55 (2010) 3109–3117.
[33] D. Fang, K.L. Huang, S.Q. Liu, Z.J. Li, J. Alloys Compd. 464 (2008) L5–L9.
[34] L.G. Xue, Z. Wei, R. Li, J.L. Liu, T. Huang, A.S. Yu, J. Mater. Chem. 21 (2011) 3216–3220.
[35] F.X. Wu, X.H. Li, Z.X. Wang, H.J. Guo, L. Wu, X.H. Xiong, X.J. Wang, J. Alloys Compd. 509 (2011) 3711–3715.
[36] J.Y. Yan, H.H. Song, S.B. Yang, X.H. Chen, Mater. Chem. Phys. 118 (2009) 367–370.